



# The effect of radiation on the structure and ligand field of borate glasses containing Cr ions

A. I. Ismail<sup>1</sup> · A. Samir<sup>2</sup> · F. Ahmad<sup>3</sup> · L. I. Soliman<sup>4</sup> · A. Abdelghany<sup>3</sup>

Received: 12 October 2020 / Accepted: 8 January 2021

© The Author(s), under exclusive licence to Springer Science+Business Media, LLC part of Springer Nature 2021

## Abstract

A glass system of composition  $[(50-x) \text{B}_2\text{O}_3-25\text{ZnO}-25\text{Na}_2\text{O}-x\text{Cr}_2\text{O}_3]$ , where ( $x=0.0, 0.1, 0.3, 0.5$  mol.%) was synthesized applying traditional melt quenching technique. The amorphous nature of the samples was proved using X-ray diffraction. The effect of Cr ion content and  $\gamma$  ray irradiation on the optical, ESR, and FTIR spectra were studied. The optical absorption spectra were carried out and a ligand field theory analysis was studied, utilizing the resulting data. Through the analysis, the crystal field energy (10Dq), Racah parameters (B and C), and nephelauxetic function (h) were calculated. The results reveal that a strong crystal field strength around chromium ions. The obtained ESR signals pointed to both  $\text{Cr}^{6+}$  and  $\text{Cr}^{3+}$  states are present in the host borate glass. FTIR spectra showed a minor variation in the intensities of some absorption peaks after radiation. It can be connected to either some limited changes in the bond angles or bond lengths within the borate glass matrix. The effect of the  $\gamma$  irradiation on the structural properties of prepared samples has no remarkable change, so the obtained samples are more stables against  $\gamma$  irradiation.

**Keywords** Borate glasses ·  $\gamma$  irradiation · Optical properties · Ligand field · ESR · FT-IR

---

✉ A. Samir  
ahmed.soliman01@feng.bu.edu.eg

✉ F. Ahmad  
fatma.ahmed@azhar.edu.eg

L. I. Soliman  
ahmed.soliman01@feng.bu.edu.eg

<sup>1</sup> Physics Department, Modern Academy for Engineering and Technology in Maadi, Cairo, Egypt

<sup>2</sup> Engineering Mathematics and Physics Department, Faculty of Engineering At Shoubra, Benha University, Cairo 11629, Egypt

<sup>3</sup> Physics Department, Faculty of Science, Al-Azhar University (Girls Branch), Cairo 11754, Egypt

<sup>4</sup> National Research Centre, DokkiCairo 12622, Egypt

## 1 Introduction

Because of the unique properties of glasses (e.g. hardness, good strength, transparency, and excellent corrosion), there is an increasing interest in glasses. Borate glasses are characterized by their particular structure and physical features, as well as being inorganic hosts for transition materials; therefore, borate glasses are receiving special attention. In the last years, technological applications have initiated great concern in the oxide glasses studies, which contain transition metal ions (Hassan et al. 2018; Ahmad and Nabhan 2019; Farouk et al. 2020; Pal et al. 2011; Singh et al. 2004). Studies reveal nonlinear behavior, offering applications in solid-state devices, electro-optic switches, electric and electro-optical devices, and nonlinear optical parametric converters (Nazabal et al. 2001). Because of the highly sensitive response of transition metal ions to the changes in the surrounding cations and their ability to have more than one valance state, transition metal ions are known to impact the optical, electrical, and magnetic properties of glasses. These ions can also be a broad radial distribution of outer d-orbital electron functions and they have a highly sensitive response to the surrounding cations (Pascuta et al. 2008; Ravikumar et al. 2003). To characterize the local structure of glasses, transition metal ions are incorporated into glasses as spectroscopic probes. These studies involve many aspects, for example, the glasses network geometry of structural units, the chemical bonds character in glasses as well as the transition metal ions coordination local symmetry and its change with the glass composition (Ravikumar et al. 2003). Chromium is particularly a paramagnetic ion, as it exists in various oxidation states ( $\text{Cr}^{2+}$ ,  $\text{Cr}^{3+}$ ,  $\text{Cr}^{4+}$ ,  $\text{Cr}^{5+}$ , and  $\text{Cr}^{6+}$ ). Eventually, a mixed-valence like this is, can be connected to its role, by being either a glass former or modifier (Mohan et al. 2008; Silva et al. 2013; Kesavulu et al. 2010; Pisarski et al. 2009; Meejitpaisan et al. 2012; Giridhar et al. 2011; Terczynska-Madej et al. 2011; Kanth et al. 2005; Hassan et al. 2012). Chromium ions dissolved in glasses; color these glasses, and they also have a strong effect on the insulating character and optical transmission of these glasses as well. Currently, remarkable attention has been given to the study of oxide glasses doped with transition metal ions (TMI) due to their attractive combination of physical and chemical properties. TMI doped borate glasses have several applications in different fields such as microelectronics, optical glasses, and solid-state laser (Kesavulu et al. 2010; Pisarski et al. 2009; Meejitpaisan et al. 2012; Murth et al. 2000). The present work aims to obtain a new family of borate glasses containing Cr ions to be more stable against  $\gamma$ -radiation and confirm their ability to shield  $\gamma$  radiation. Additionally, the effects of adding  $\text{Cr}_2\text{O}_3$  on borate glasses and the ligand field are presented.

## 2 Experimental details

Conventional melt quenching technique has been used to prepare a borate glassy system of composition  $(50-x) \text{B}_2\text{O}_3\text{-}25\text{ZnO-}25\text{Na}_2\text{O-}x\text{Cr}_2\text{O}_3$  where ( $x=0.0, 0.1, 0.3, 0.5$  mol.%). The raw materials used to prepare the glasses of present work are  $\text{H}_3\text{BO}_3$ ,  $\text{ZnO}$ ,  $\text{Cr}_2\text{O}_3$ , and  $\text{Na}_2\text{CO}_3$  with 99.9% of purity. The composition of each sample was heated in an electric furnace at (700 °C) for 10 min to liberate the gases from the molten. The temperature of the furnace has been raised to (950 °C) for 40 min. The molten was then poured between two polished copper blocks. These two polished copper blocks were preserved at room temperature to produce the homogeneous glasses.

X-ray diffraction (XRD) measurements are performed using (Philips–PW3719) diffractometer with Cu-K $\alpha$  X-ray beam with a wavelength of 1.542 Å. X-ray diffraction patterns were recorded in  $2\theta$  ranging between 4 to 90° with a scanning rate 2 degrees/min. The prepared samples density was measured by applying Archimedes principle using carbon tetrachloride (density 1.592 g/cm<sup>3</sup>) as an immersion liquid. The Fourier-Transform infrared absorption spectra were recorded using (FT-IR Perkin Elmer) in the range 1600–400 cm<sup>-1</sup>, using the KBr pellet technique. For FITR measurements the powder-samples were mixed with high purity KBr and pressed into discs. The sample-to-KBr ratio was kept at ~3% for all samples. Irradiation of the glass samples was performed using a <sup>60</sup>Co gamma source (Gamma chamber 4000 A, manufactured by Atomic Energy Agency of Egypt). The dose rate for irradiation was ranging from 2.4787 to 2.279 kGy/hr. The glass samples were irradiated for the necessary time interval to achieve the desired overall dose. The optical absorption spectra of the samples were recorded at room temperature using a UV–Vis spectrophotometer, JENWAY 6405 UV/Vis in the range from 250 to 850 nm. The glass flakes used in the measurements were larger than (10 × 10) mm<sup>2</sup> and have a thickness of ~0.5 mm. ESR spectra were measured on an ESR spectrometer (EMX Bruker) operating in X-band frequency at room temperature for all the samples. The magnetic field was scanned from 75 to 6000 Gauss.

### 3 Results and discussion

#### 3.1 X-Ray diffraction

The obtained glass samples were firstly checked by X-Ray diffraction. The X-ray charts of the prepared glasses in the powder form are shown in Fig. 1. The diffraction charts show no sharp peaks indicating (non-crystalline nature) of the prepared samples (Hassan 2013). Moreover, the patterns exhibit abroad hump at ( $2\theta \sim 30^\circ$ ), which is a typical feature of borate glasses (Ahmad 2014).

#### 3.2 Density and molar volume

Both the density and molar volume are intrinsic properties that are related directly to other properties such as thermal expansion, heat capacity, compactness, crosslink densities, geometrical configuration, and interstitial spaces dimensions of the glass. As a result, when the light elements are replaced by other heavy elements in any glass, this in turn, increases the density that has a linear dependence on doping content. The dependence of the density obtained results, as well as the calculated molar volume  $V_M$  on Cr<sub>2</sub>O<sub>3</sub> content for the samples, are illustrated in Fig. 2. These results have revealed; that as the chromium oxide ratio increased, the density increased. This is most probably due to the replacement of B<sub>2</sub>O<sub>3</sub> (atomic mass 69.62 g/mol.) by Cr<sub>2</sub>O<sub>3</sub> (atomic mass 151.99 g/mol.). It has also been declared that the molar volume has been decreased with increasing the Cr<sub>2</sub>O<sub>3</sub> content; this indicates the existence of a compact structure with less polymerization due to the shortened chain which confirmed that the glass network became compactable. The glass density and its molar volume follow the normal behavior trend, which can be considered as an opposite one (Uma et al. 2006; Singh et al. 2011).

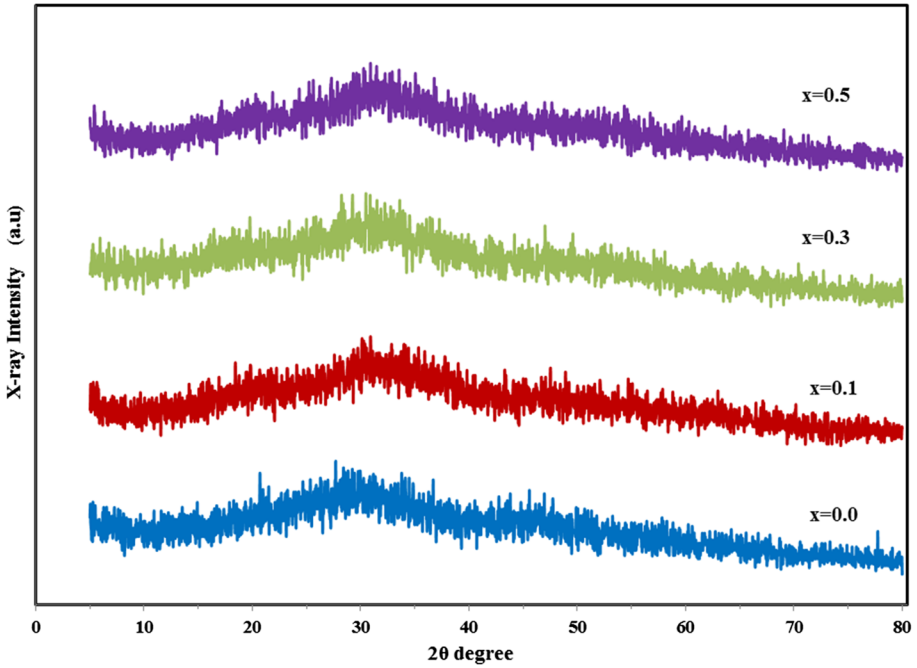


Fig. 1 X-Ray diffraction pattern of the investigated samples

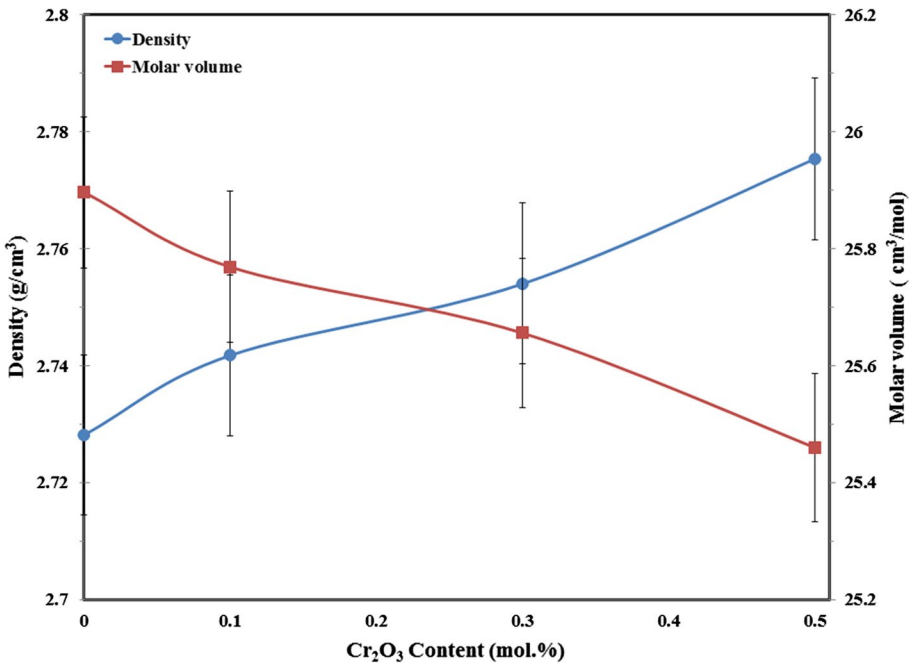


Fig. 2 The dependence of density and molar volume on (Cr<sub>2</sub>O<sub>3</sub>) content

### 3.3 Oxygen packing density

The density of oxygen packing (OPD) which can be defined as a measure of the tightness of the oxide network packing, is calculated using molecular weight ( $M_w$ ) of the glass samples and their density ( $\rho$ ) according to the relation mentioned below (Farouk et al. 2013):

$$O = (\rho / M_w)n \quad (1)$$

where  $n$  represents the oxygen atoms number per formula unit. The estimated values of oxygen packing density are found to be 77.23, 77.39, 77.61 and 77.79 mol./l for  $x=0.0$ , 0.1, 0.3, 0.5 mol. %, respectively. Such an increase indicates to the structure becomes highly packed. It confirms the formation of non-bridging oxygen NBOs with increasing  $Cr_2O_3$  content, which agrees with FTIR measurements later (Moustafa et al. 2014).

### 3.4 UV-Vis spectroscopy

Figure 3 describes the optical absorption spectra of Cr ions doped glasses before and after irradiation. It can be observed that the absorption edge is not sharp which confirms that the prepared compositions are glassy in nature and is in agreement with the XRD measurements. There is no disappeared or added band after irradiation related to some shielding effect of Cr ions where it causes the blocking of the free transit or transfer of the loosed electrons during the irradiation process. The slight increase in absorption

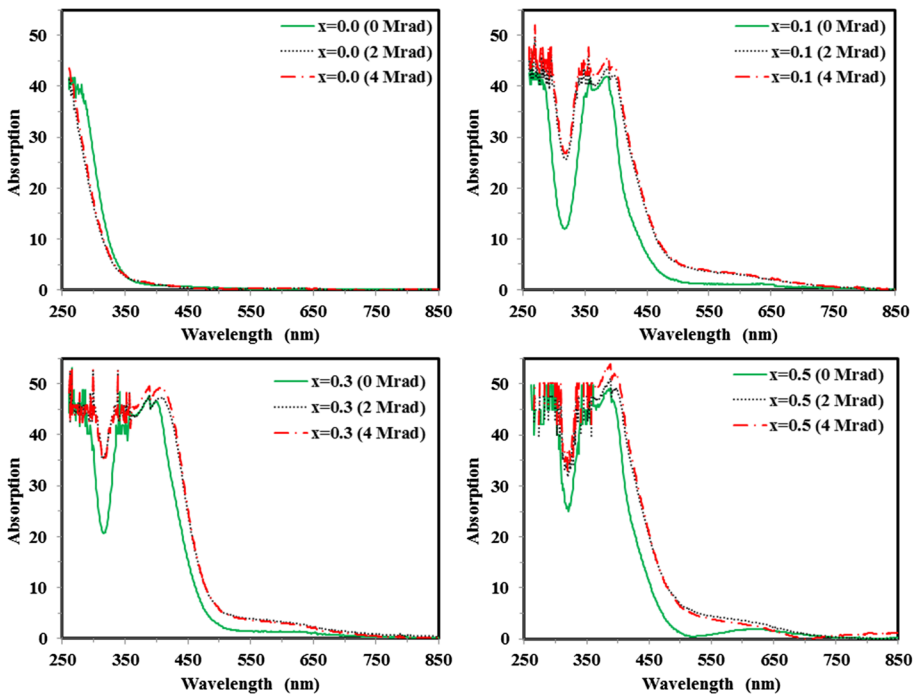


Fig. 3 Optical absorption spectra of the investigated samples before and after radiation

bands intensity of irradiated samples may be due to photochemical reactions between the 3d Cr ions.  $\gamma$  irradiation produced electrons and/or positive holes during irradiation. Cr ions can absorb the excited electrons or pick up the liberated holes and subsequently are changed to lower or higher valence states ( $\text{Cr}^{3+}$ ,  $\text{Cr}^{6+}$ ), respectively. Therefore, they share in the shielding process (El et al. 2020; El Batal et al. 2014; Abdelghany et al. 2012).

On the other hand, the researches of optical absorption glasses doped with transition metals lead to the ligand field of absorption energies, which in turn reflect the octahedral and tetrahedral coordination distortion. The samples spectrum exhibits two main absorption bands at  $\sim 598$  ( $\nu_1$ ) and  $426$  ( $\nu_2$ ) nm; that can be determined due to the conventional transitions of  $\text{Cr}^{3+}$  ions (Kesavulu et al. 2010; Batal et al. 2008). The spectra have been analyzed and the bands have also been assigned as well to  ${}^4\text{A}_{2g} \rightarrow {}^4\text{T}_{2g}$  and  ${}^4\text{A}_{2g} \rightarrow {}^4\text{T}_{1g}$  transitions respectively, which in turn refer to d–d transition of  $\text{Cr}^{3+}$  ion. The colors of the prepared samples are yellow-green indicating a trivalent chromium oxidation state (Pisarski et al. 2009). Furthermore,  $\text{Cr}^{6+}$  ion is identified by the absorption of the charge transfer in the UV range around  $\sim 390$  and  $348$  nm which is attributed to  ${}^4\text{A}_{2g} \rightarrow {}^2\text{A}_{1g}$  and  ${}^4\text{A}_{2g} \rightarrow {}^2\text{T}_{1g}$  (P) transition, respectively. The average sum of the chromium hexavalent bands position is represented by ( $\nu_3$ ). This is most probably caused by the contribution of the chromium ions in a higher valence state ( $\text{Cr}^{6+}$ ), which is not d–d transition (Hassan et al. 2018; Flower et al. 2007). The intensity of absorption bands increases with increasing  $\text{Cr}_2\text{O}_3$  content.

The ligand field parameters, as crystal field strength (10Dq) which represents the crystal field splitting energy, and the Racah parameters (B and C) that measure the inter-electronic repulsion among the 3d electrons of chromium ion, has been calculated from the spectral band absorption positions ( $\nu_1$ ,  $\nu_2$ ,  $\nu_3$  in  $\text{cm}^{-1}$ ) using the relations (Hassan et al. 2012):

$$10Dq = \nu_1 \quad (2)$$

$$B = \frac{(2\nu_1 - \nu_2)(\nu_2 - \nu_1)}{(27\nu_1 - 15\nu_2)} \quad (3)$$

$$C = \frac{\nu_3 - 4B - \nu_1}{3} \quad (4)$$

Figure 4 illustrates the ligand field parameters values (Dq, B, C, and Dq/B) that have been got before and after irradiation. It is obvious that the crystal field Dq increases with the increase in  $\text{Cr}_2\text{O}_3$  content. On the other hand, the Racah parameters B and C values follow the opposite trend. The data here propose that the environment of the chromium ion is more covalence, and larger numbers of electrons are delocalized on the d-shell (Kesavulu et al. 2010; Rao and Veeraiah 2002). The ratio Dq/B describes crystal-field strength. It was found that the value of Dq/B was more than 2.3 in the strong crystal-field sites, much less than 2.3 in the weak field, and finally close to 2.3 in the intermediate fields (Pisarski et al. 2009). The acquired value of the ratio Dq/B reflects the strong crystal field strength around chromium ions. The relation between Racah parameters (C/B ratio), namely  $C=4B$ , is acceptably satisfied (i.e.,  $C=3.9 B \pm 0.4$ ) as shown in Table 1. Additionally, the Racah parameters are used in defining the degree of ionicity of the ligand bonding, the bonding formation (or nephelauxetic ratio h) was also evaluated using the following formula (Ahmad 2014):

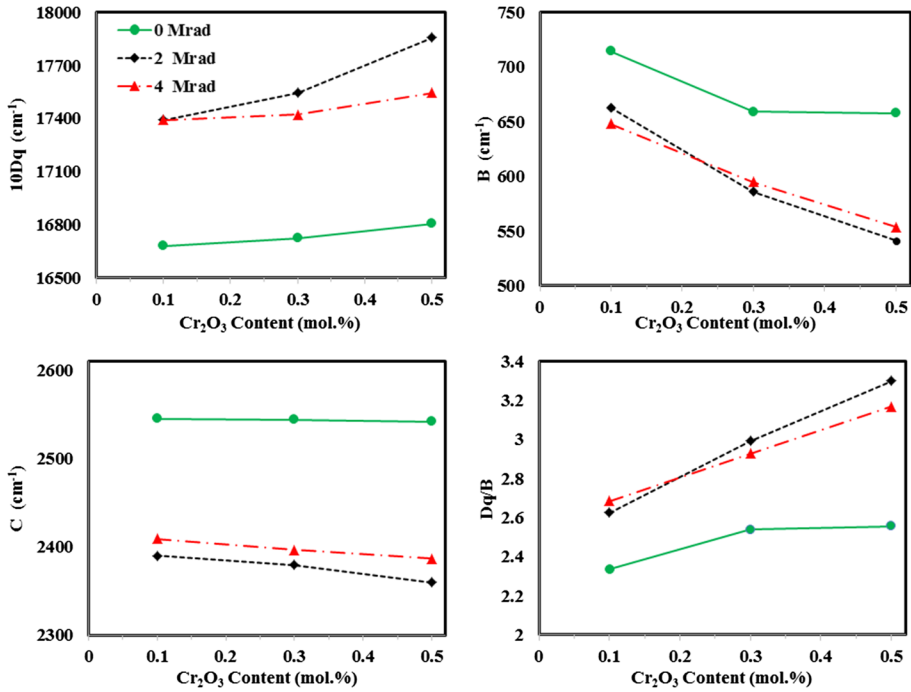


**Fig. 4** The ligand field parameters values (Dq, B, C and Dq/B) before and after irradiation as a function of (Cr<sub>2</sub>O<sub>3</sub>) content

$$h = \frac{[(B_{free} - B)/B_{free}]}{K_{Cr^{3+}}} \tag{5}$$

where  $B_{free} = 918 \text{ cm}^{-1}$  is the value of the free (gaseous)  $\text{Cr}^{3+}$  ion, the central metal ion, where its value is  $k_{Cr^{3+}} = 0.21$ . The obtained values of  $h$  for all the investigated glasses before and after radiation show the same behavior as Dq (Table 1). The nephelauxetic function  $h$  values became higher with the increase of  $\text{Cr}_2\text{O}_3$  content, which suggests the raise in covalent bond in the glass matrix. The increment of  $h$  values refers to a decrease in the d-electrons localization, which can be related to the d orbitals overlapping with ligand orbitals (Ahmad and Nabhan 2019).

The study of the fundamental absorption edge in the UV region is a useful method for the investigation of optical transitions and their correlation with the electronic band structure in amorphous materials. The optical band gap energy values  $E_g$  were obtained according to equation (Hassan et al. 2018; El-Fattah et al. 2017; Ahmad et al. 2014):

$$ah\nu = A(h\nu - E_g)^n \tag{6}$$

where  $n=2$  for indirect allowed band transition model for the glassy samples. The plots of  $(\alpha h\nu)^{1/2}$  as a function of photon energy  $h\nu$  are shown in Fig. 5. The figure presents an example for such linear regions defining the absorption edges and the corresponding linear fittings applied to the before radiation samples for an accurate estimation of the optical band gap. The gap size is estimated from the straight-line portion of this plot, as shown in the inset. From the spectra in Fig. 5, it is clear that the absorption edge shifted towards a

**Table 1** C/B, nephelauxetic ratio h,  $E_g$  and  $E_t$  values of Cr doped borate glasses at different  $\gamma$  radiation doses

$x$ (mol. %)	C/B				h				$E_g$ (eV)				$E_t$ (eV)					
	0 Mrad		2 Mrad		4 Mrad		0 Mrad		2 Mrad		4 Mrad		0 Mrad		2 Mrad		4 Mrad	
0.0	–	–	–	–	–	–	–	–	–	–	–	–	–	–	–	–	–	–
0.1	3.56	3.61	3.72	3.72	1.06	1.32	1.40	3.41	3.28	3.29	3.29	3.28	3.05	2.92	0.26	0.31	0.37	
0.3	3.86	4.06	4.03	4.03	1.34	1.72	1.68	3.59	2.56	2.47	2.47	2.56	2.47	0.28	0.33	0.36	0.41	
0.5	3.87	4.36	4.31	4.31	1.35	1.95	1.89	3.38	2.47	2.27	2.27	2.47	2.27	0.31	0.38	0.38	0.42	



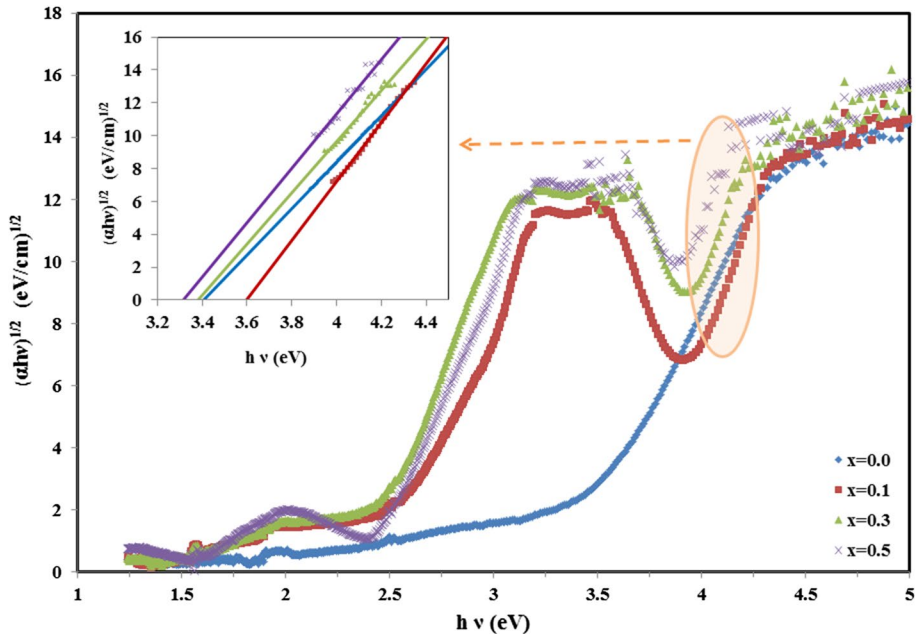


**Fig. 5**  $(\alpha h\nu)^{1/2}$  as a function of photon energy  $h\nu$  applied to the experimental data before radiation. The upper inset highlights the respective straight-line portions

higher wavelength with increasing of  $\text{Cr}_2\text{O}_3$  content. The obtained values of  $E_g$  before and after radiation represented in Table 1, decrease with the increasing of the  $\text{Cr}_2\text{O}_3$  content.

The Urbach energy  $E_t$  can be evaluated from the relation (El-Fattah et al. 2017; Ahmad et al. 2014):

$$\alpha(\omega) = \alpha_o \exp(h\nu/E_t) \quad (7)$$

Urbach energy is used to characterize the degree of disorder in glassy systems as dangling bonds and non-bridging oxygens NBOs. The  $E_t$  values of the present samples are increasing (Table 1).

The decrease in  $E_g$  and increase in  $E_t$  values with increasing of  $\text{Cr}_2\text{O}_3$  content is possibly attributed to the presence of chromium ions in the state of  $\text{Cr}^{3+}$  which acts as modifiers, yield increase in the degree of disorder and NBOs concentration in the glass matrix, which agrees with FTIR measurements later (Ravikumar et al. 2003; Hassan et al. 2012). While after irradiation it may be due to an increased number of defects upon  $\gamma$  irradiation by breaking bonds and or/ making some atomic displacements (El et al. 2020; Moustafa et al. 2013; Sallam et al. 2020). Effect of  $\gamma$ -radiation on the calculated optical parameters of the glasses sample appears good stability accompanying with small variations.

### 3.5 ESR spectroscopy

Figure 6 represents ESR spectra for the investigated glass system doped with  $\text{Cr}_2\text{O}_3$  before and after radiation dose (4 Mrad). The undoped sample ( $x=0\%$ ) reveals observed signal at 1677 G ( $g \sim 4.11$ ) are related to the presence of inevitable trace  $\text{Fe}^{3+}$  ions impurities within

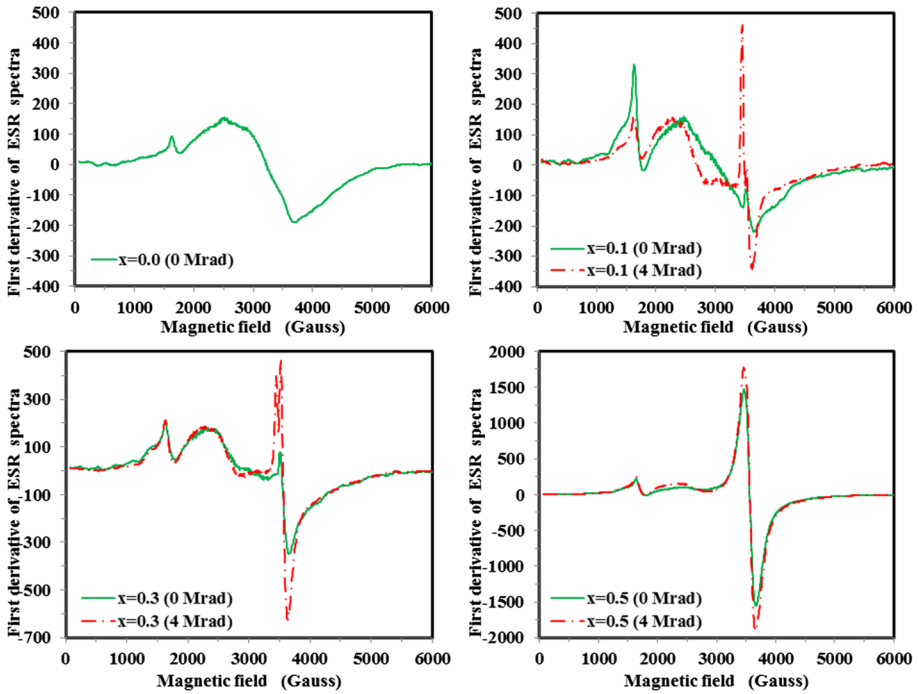


Fig. 6 ESR spectra for the investigated samples before and after radiation dose (4 Mrad)

the raw materials used for the preparation of investigated glasses (Giridhar et al. 2011; El Batal et al. 2014). In samples containing Cr ions, the resonance line at a low magnetic field at 1431 G ( $g \sim 4.82$ ) is attributed to isolated  $\text{Cr}^{3+}$  ions in distorted octahedral sites subjected to strong crystal field effects (Hassan et al. 2018; Narendrudu et al. 2017; Krishna et al. 2007). The resonance contributes intense absorption line ( $g \sim 4.11$ ) is referred to  $\text{Cr}^{3+}$ , even though  $\text{Fe}^{3+}$  impurities may be at the source of this band (Hassan et al. 2019). Likewise, a broad resonance line with  $g \sim 2.21$  is observed which has been assigned to exchange-coupled pairs or large clusters of  $\text{Cr}^{3+}$  (Hassan et al. 2018; Singh et al. 2009).

All spectra exhibit a strong signal located at  $g \sim 1.93$ , which is due to the presence of  $\text{Cr}^{5+}$  ions which exist naturally and produced after the charge transfer between  $\text{Cr}^{6+}$  and  $\text{O}^{2-}$  (Hassan et al. 2018; Flower et al. 2007; Madej et al. 2010). The large intensity of this resonance signal indicates higher concentrations of  $\text{Cr}^{6+}$  ions in this glass network. The intensity of  $\text{Cr}^{6+}$  signal was improved noticeably after irradiation, which agrees with optical measurements. ESR spectra reveal that host glasses favor the presence of Cr ions in higher valence states (network former) due to increase the bonding defects (El Batal et al. 2014; Abdelghany et al. 2012).

### 3.6 FTIR studies

The IR spectra have been widely used to get information about the local symmetry of different materials and structural units in glassy systems. Figure 7 represents the IR absorption spectrum of samples before and after radiation dose (4 Mrad). It was

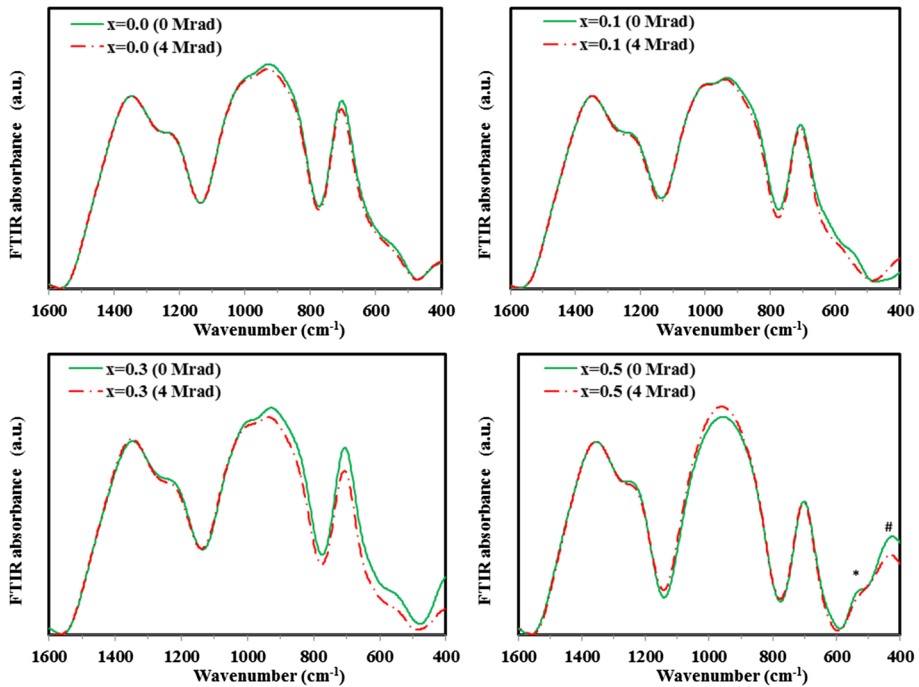


**Fig. 7** The IR spectra of the investigated samples before and after radiation dose (4 Mrad)

assumed that an absorption band in IR spectra may be due to the vibration of either atomic vibration or function group in the network. This concept was successfully applied in many studies concerning glassy materials (Dimitriev et al. 1979; Dimitrov and Dimitriev 1990). The borate network vibration modes are mainly active in three IR spectral regions. These three regions can be classified as follows: (i) the first one from 1200 to 1600  $\text{cm}^{-1}$ , (ii) the second; from 800 to 1200  $\text{cm}^{-1}$ , and (iii) the third from 600 to 800  $\text{cm}^{-1}$ . The region which, is attributed to the stretching and relaxation of the B-O bond of the trigonal  $\text{BO}_3$  units is the first band. On the other side, the second region is attributed to  $\text{BO}_4$  units, while the third one is caused by the bending of B-O-B linkages in the borate network (Samir et al. 2019; Reddy and Veeraiah 2000). Under the presence of Zn-O tetrahedral bending vibrations of  $\text{ZnO}_4$  units, the observed shoulder at  $\sim 550 \text{ cm}^{-1}$  (El-Zaiat et al. 2016; Raju et al. 2006). Absorption band is observed at less than  $\sim 460 \text{ cm}^{-1}$  (marked by #) may be related to  $\text{Na}^+$  modifying site vibrations (Farouk et al. 2019). A weak absorption band is observed at  $\sim 460 \text{ cm}^{-1}$  (marked by\*) at higher content of  $\text{Cr}_2\text{O}_3$ , which may due to the presence of Cr ions in hexavalent state  $\text{Cr}^{6+}$  (tetrahedral coordination) (Hassan et al. 2018). Also, the IR spectra of radiated samples under the study have revealed almost the same spectral features as those before irradiation with minor variations in the intensities of some absorption peaks. It can be connected to either some limited changes in the bond angles or bond lengths in borate units arrangement (Moustafa et al. 2013; Sallam et al. 2020; El Batal et al. 2009). The observed maintenance of the main vibrational bands features which, is due to both triangular and tetrahedral borate groups upon  $\gamma$  irradiation, could be attributed to the

stability of those constitutional building units as being uninfluenced by irradiation. To get information of the unit's formation in the borate structure, the bands were studied by deconvoluted for the spectra of the samples (Pascuta et al. 2009). The broad bands are most probably a result of the overlapping of individual bands. The deconvolution for the IR spectrum bands was done by using Gaussian line shapes. As a result,  $N_4$  can be defined as the ratio of the  $BO_4$  units to the total ( $BO_3 + BO_4$ ) units (Pascuta et al. 2008; Kuang et al. 2017; Saddeek et al. 2008; Moustafa et al. 1996). The values of  $N_4$  plotted against Cr ions concentration before and after irradiation dose (4 Mrad) as shown in Fig. 8. It is clear that  $N_4$  ratio shows a tendency to decrease with increasing the Cr ions concentration. This allows us to assume that increasing  $Cr_2O_3$  ions cause changes in the structural units and formation of NBO in the glass matrix. It may be due to the increase of  $Cr^{3+}$  ions that act as modifiers (octahedral coordination). The observed limited decrease in  $N_4$  after irradiation may be due to the generation of induced structural defects in the glass matrix by breaking bonds (Moustafa et al. 2013; Sallam et al. 2020).

## 4 Conclusions

The investigated samples of borate glasses containing Cr ions are amorphous as confirmed by X-ray diffraction. It is observed that the density increase by the increase of Cr content, on the contrary, the molar volume follows the opposite behavior.  $Dq$  increases with the increase of  $Cr_2O_3$  content. While both of the Racah parameters B and C values follow a

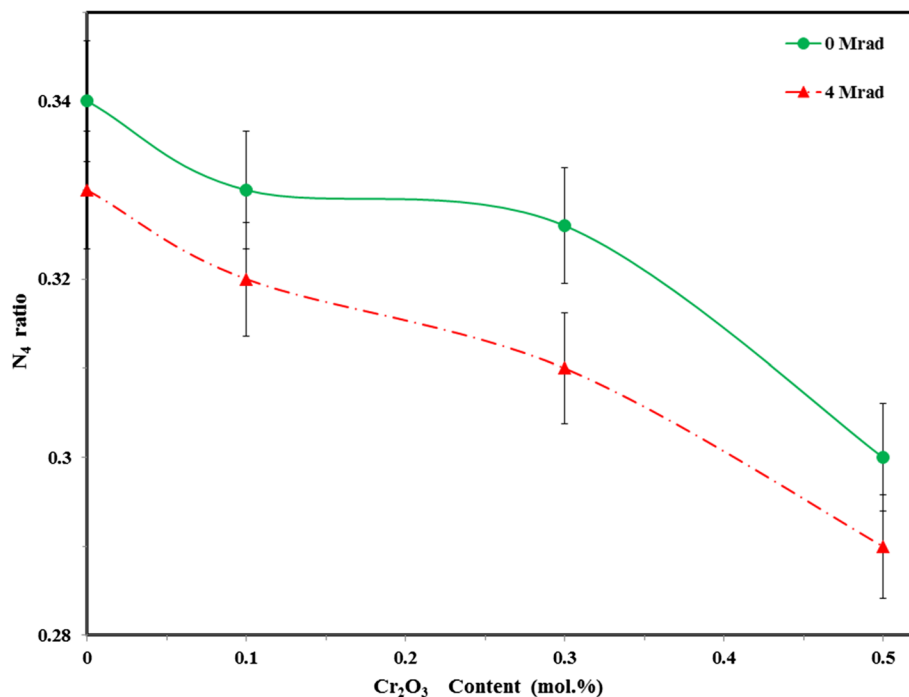


Fig. 8 Variation of  $N_4$  ratio before and after radiation dose (4 Mrad)

reverse behavior. The environment of the chromium ion is more covalence, and larger numbers of electrons are delocalized on the d-shell. Optical and ESR spectra confirm that the present hexavalent and trivalent Cr ions within the host glass matrix. The FTIR absorption spectra showed almost no change in the position of most absorption bands. So the obtained samples are more stables against  $\gamma$  irradiation.

**Acknowledgements** The authors would like to acknowledge Prof. Dr. Moukhtar A. Hassan, Physics Department, Faculty of Science, Al-Azhar University, for his active sharing in the discussion of the manuscript and for providing laboratory facilities.

**Funding** This publication and there has been no significant financial support for this work that could have influenced its outcome.

## Compliance with ethical standards

**Conflict of interest** The authors declare that they have no competing interests.

## References

- Abdelghany, A.M., El Batal, F.H., Azooz, M.A., Ouis, M.A., El Batal, H.A.: Optical and infrared absorption spectra of 3D transition metal ions-doped sodium borophosphate glasses and effect of gamma irradiation. *Spectrochim Acta Part A Mol. Biomol. Spectrosc.* **98**, 148–155 (2012)
- Ahmad, F.: Study the effect of alkali/alkaline earth addition on the environment of borochromate glasses by means of spectroscopic analysis. *J. Alloys Comp.* **586**, 605–610 (2014)
- Ahmad, F., Nabhan, E.: Spectroscopic and mechanical studies of lithium aluminoborate glasses doped with chromium ions. *Opt. Quant. Electron.* **51**, 261 (2019)
- Ahmad, F., Aly, E.H., Atef, M., Elokr, M.M.: Study the influence of zinc oxide addition on cobalt doped alkaline earth borate glasses. *J. Alloys Comp.* **593**, 250–255 (2014)
- da Silva, M.A.F.M., Carvalho, I.C.S., Cellac, N., Bordallo, H.N., Sosman, L.P.: Evidence of broad emission band in the system  $\text{MgGa}_2\text{O}_4\text{-Ga}_2\text{O}_3$  doped with  $\text{Cr}^{3+}$  ions. *Opt. Mater.* **35**(3), 543–546 (2013)
- Dimitriev, Y., Dimitrov, V., Arnaudov, M.: IR spectra and structure of tellurite glasses. *J. Mater. Sci.* **14**, 723–727 (1979)
- Dimitrov, V., Dimitriev, Y.: Structure of glasses in  $\text{PbO-V}_2\text{O}_5$  system. *J. Non. Cryst. Solids* **122**, 133–138 (1990)
- El Batal, F.H., El Kheshen, A.A., Azooz, M.A., Abo-Naf, S.M.: Gamma ray interaction with lithium diborate glasses containing transition metals ions. *Opt. Mater.* **30**, 881–891 (2008)
- El Batal, F.H., Hamdy, Y.M., Marzouk, S.Y.: UV-visible and infrared absorption spectra of transition metals-doped lead phosphate glasses and the effect of gamma irradiation. *J. Non Cryst. Solids.* **355**, 2439–2447 (2009)
- El Batal, H.A., Hussein, E.M.A., ElAlaily, N.A., Ezz-Eldin, F.M.: Effect of different 3D transition metal oxides on some physical properties of  $\gamma$ -Irradiated  $\text{Bi}_2\text{O}_3\text{-B}_2\text{O}_3$  glasses: a comparative study. *J. Non Cryst. Solids* **528**, 119733 (2020)
- El Batal, F.H.A., Marzouk, M.A., Hamdy, Y.M., El Batal, H.A.: Optical and FT infrared absorption spectra of 3D transition metal ions doped in  $\text{NaF-CaF}_2\text{-B}_2\text{O}_3$  glass and effects of gamma irradiation. *J. Solid State Phys.* **2014**, 3899543 (2014)
- El-Fattah, Z.M.A., Ahmad, F., Hassan, M.A.: Tuning the structural and optical properties in cobalt oxide-doped borosilicate glasses. *J. Alloys Comp.* **728**, 773–779 (2017)
- El-Zaiat, S.Y., Medhat, M., Omar, M.F., Shirif, M.A.: Effect of UV exposure on photochromic glasses doped with transition metal oxides. *Opt. Commun.* **370**, 176–182 (2016)
- Farouk, M., Samir, A., Metawe, F., Elokr, M.: Optical absorption and structural studies of bismuth borate glasses containing Er ions. *J. Non Cryst. Solids.* **371**, 14–21 (2013)
- Farouk, M., Ahmad, F., Samir, A.: Ligand field and spectroscopic investigations of cobalt doped erbium-zinc borate glasses. *Opt. Quant. Electron.* **51**, 292 (2019)
- Farouk, M., Slibi, D.-A., El-Fattah, Z.M.A., Atallah, M., El-Sherbiny, M.A., Hassan, M.A.: Effect of  $\text{SiO}_2$  Addition on Chromium Transitions in Borate Glasses. *Silicon.* **5**, 1–8 (2020)

- Flower, G.L., Reddy, M.S., Baskaran, G.S., Veeraiiah, N.: The structural influence of chromium ions in lead gallium phosphate glasses by means of spectroscopic studies. *Opt. Mater.* **30**, 357–363 (2007)
- Giridhar, G., Sastry, S.S., Rangacharyulu, M.: Spectroscopic studies on  $\text{Pb}_3\text{O}_4\text{-ZnO-P}_2\text{O}_5$  glasses doped with transition metal ions. *Phys. B Condensed Matter.* **406**, 4027–4030 (2011)
- Hassan, M.A.: Effect of halides addition on the ligand field of chromium in alkali borate glasses. *Alloys Comp.* **574**, 391–397 (2013)
- Hassan, M.A., Farouk, M., Abdullah, A.H., Kashef, I., ElOkr, M.M.: ESR and ligand field theory studies of  $\text{Nd}_2\text{O}_3$  doped borochromate glasses. *J. Alloys Comp.* **539**, 233–236 (2012)
- Hassan, M.A., Ahmad, F., El-Fattah, Z.M.A.: Novel identification of ultraviolet/ visible  $\text{Cr}^{6+}/\text{Cr}^{3+}$  optical transitions in borate glasses. *J. Alloys Compd.* **750**, 320–327 (2018)
- Hassan, M.A., Ebrahim, F.M., Moustafa, M.G., Abd El-Fattah, Z.M., El-Okr, M.M.: Unraveling the hidden Urbach edge and  $\text{Cr}^{6+}$  optical transitions in borate glasses. *J. Non Cryst. Solids.* **515**, 157–164 (2019)
- Kanth, C.L., Rao, B.A., Veeraiiah, N.: Veeraiiah, Spectroscopic investigations on  $\text{ZnF}_2$  MO– $\text{TeO}_2$  (MO=ZnO, CdO and PbO) glasses doped with chromium ions. *J. Quant. Spectrosc. Radiat. Transfer.* **90**, 97–113 (2005)
- Kesavulu, C.R., Chakradhar, R.P.S., Jayasankar, C.K., Rao, J.L.: EPR, optical, photoluminescence studies of  $\text{Cr}^{3+}$  ions in  $\text{Li}_2\text{O-Cs}_2\text{O-B}_2\text{O}_3$  glasses-an evidence of mixed alkali effect. *J. Mol. Struct.* **975**, 93–99 (2010)
- Krishna, G.M., Kumari, B.A., Reddy, M.S., Veeraiiah, N.: Characterization and physical properties of  $\text{Li}_2\text{O-CaF}_2\text{-P}_2\text{O}_5$  glass ceramics with  $\text{Cr}_2\text{O}_3$  as a nucleating agent—physical properties. *J. Solid State Chem.* **180**, 2747–2755 (2007)
- Kuang, M.-Q., Wang, L.-D., Duan, S.-K.: Local distortion and EPR parameters of copper(II) in borate glasses. *J. Phys. Chem. Solids.* **111**, 41–46 (2017)
- Madej, A.T., Kowalska, K.C., Laczka, M.: The effect of silicate network modifiers on colour and electron spectra of transition metal ions. *Opt. Mater.* **32**, 1456–1462 (2010)
- Meejitpaisan, P., Kaewkhao, J., Limsuwan, P., Kedkaew, C.: Physical and optical properties of the SLS glass doped with low  $\text{Cr}_2\text{O}_3$  concentrations. *Proc. Eng.* **32**, 787–392 (2012)
- Mohan, S., Thind, K.S., Sharma, G., Gerward, L.: Spectroscopic investigations of  $\text{Nd}^{3+}$  doped fluoro- and chloro-borate glasses. *Spectrochim Acta Part A Mol Biomol. Spectrosc.* **70**, 1173–1179 (2008)
- Moustafa, Y.M., Hassan, A.K., Damrawi, G.E.L., Yevtushenko, N.G.: Structural properties of  $\text{V}_2\text{O}_5\text{-Li}_2\text{O-B}_2\text{O}_3$  glasses doped with copper oxide. *J. Non Cryst. Solids* **194**, 34–40 (1996)
- Moustafa, F.A., Fayad, A.M., Ezz-Eldin, F.M., El-Kashif, I.: Effect of gamma radiation on ultraviolet, visible and infrared studies of  $\text{NiO}$ ,  $\text{Cr}_2\text{O}_3$  and  $\text{Fe}_2\text{O}_3$ -doped alkali borate glasses. *J. Non Cryst. Solids.* **376**, 18–25 (2013)
- Moustafa, F.A., Abdel-Baki, M., Fayad, A.M., El-Diasty, F.: Role of mixed valence effect and orbital hybridization on molar volume of heavy metal glass for ionic conduction pathways augmentation. *Am J. Mater. Sci.* **4**(3), 119–126 (2014)
- Murth, M.K., Murthy, K.S.N., Veeraiiah, N.: Dielectric properties of  $\text{NaF-B}_2\text{O}_3$  glasses doped with certain transition metal ions. *Bull. Mater. Sci.* **23**, 285–293 (2000)
- Narendrudu, T., Suresh, S., Ram, G.C., Veeraiiah, N., Rao, D.K.: Spectroscopic and structural properties of  $\text{Cr}^{3+}$  ions in lead niobium germanosilicate glasses. *J. Lumin.* **183**, 17–25 (2017)
- Nazabal, V., Fargin, E., Ferreir, B., Flem, G., Desbat, B., Buffeteau, T., Couzi, M., Rodriguasz, V., Santran, S., Sargec, L.: Thermally poled new borate glasses for second harmonic generation. *J. Non Cryst. Solids.* **290**, 73–85 (2001)
- Pal, M., Roy, B., Pal, M.: Structural characterization of borate glasses containing zinc and manganese oxides. *J. Mod. Phys.* **2**, 1062–1066 (2011)
- Pascuta, P., Borodi, G., Culea, E.: Influence of europium ions on structure and crystallization properties of bismuth borate glasses and glass ceramics. *J. Non Cryst. Solids.* **345**, 5475–5479 (2008)
- Pascuta, P., Rada, S., Borodi, G., Bosca, M., Pop, L.: Eugen, Influence of europium ions on structure and crystallization properties of bismuth-alumino-borate glasses and glass ceramics. *J. Mol. Struct.* **924**, 214–220 (2009)
- Pisarski, W.A., Pisarska, J., Dominiak-Dzik, G., Ryba-Romanowski, W.: Transition metal ( $\text{Cr}^{3+}$ ) and rare earth ( $\text{Eu}^{3+}$ ,  $\text{Dy}^{3+}$ ) ions used as a spectroscopic probe in compositional-dependent lead borate glasses. *J. Alloys Comp.* **484**, 45–49 (2009)
- Raju, G.N., Veeraiiah, N., Nagarjuna, G., Satyanarayana, P.V.V.: The structural role of chromium ions on the improvement of insulating character of  $\text{ZnO-ZnF}_2\text{-B}_2\text{O}_3$  glass system by means of dielectric, spectroscopic and magnetic properties. *Phys. B Condensed Matter.* **373**, 297–305 (2006)
- Rao, G.V., Veeraiiah, N.: Study on certain physical properties of  $\text{R}_2\text{O CaF}_2\text{-B}_2\text{O}_3$ ;  $\text{Cr}_2\text{O}_3$  glasses. *J. Alloys Comp.* **339**, 54–64 (2002)

- Ravikumar, R.V.S.S.N., Kada, K.K.I., Chandrasekhar, A.V., Reddy, B.J., Reddy, Y.P., Rau, P.S.: EPR and optical studies on transition metal doped  $\text{LoRbB}_4\text{O}_7$  glasses. *J. Phys. Chem. Solids.* **64**, 261–264 (2003)
- Reddy, M., Veeraiah, S.B.R.: Optical absorption and fluorescence spectral studies of  $\text{Ho}^{3+}$  ions in  $\text{PbO}-\text{Al}_2\text{O}_3-\text{B}_2\text{O}_3$  glass system. *J. Phys. Chem. Solids.* **61**, 1567–1571 (2000)
- Saddeek, Y.B., Shaaban, E.R., El Sayed, M., Moustafa, H.M.: Spectroscopic properties, electronic polarizability, and optical basicity of  $\text{Bi}_2\text{O}_3-\text{Li}_2\text{O}-\text{B}_2\text{O}_3$  glasses. *Phys. B.* **403**, 2399–2407 (2008)
- Sallam, O.I., Ezz-Eldin, F.M., Elalaily, N.A.: Influence of doping transition metals and irradiation on some physical properties of borate glass. *J. Opt. Quant. Elect.* **52**(4), 1–20 (2020)
- Samir, A., Hassan, M.A., Abokhadra, A., Soliman, L.I., Elok, M.: Characterization of borate glasses doped with copper oxide for optical application. *Opt. Quant. Electron.* **51**, 123 (2019)
- Singh, N., Singh, K.J., Singh, K., Singh, H.: Comparative study of lead borate and bismuth lead borate glass systems as gamma-radiation shielding materials. *Nucl. Inst. Methods phys. Res. B* **225**, 305–309 (2004)
- Singh, V., Chakradhar, R.P.S., Rao, J.L., Kwak, H.-Y.: Characterization, EPR and photoluminescence studies of  $\text{LiAl}_5\text{O}_8$ : Cr phosphors. *Solid State Sci.* **11**, 870–874 (2009)
- Singh, G.P., Kaur, P., Kaur, S., Singh, D.P.: Role of  $\text{V}_2\text{O}_5$  in structural properties of  $\text{V}_2\text{O}_5-\text{MnO}_2-\text{PbO}-\text{B}_2\text{O}_3$  glasses. *Mater. Phys. Mech.* **12**, 58–63 (2011)
- Terczynska-Madej, A., Cholewa-Kowalska, K., Laczka, M.: Coordination and valence state of transition metal ions in alkali-borate glasses. *Opt. Mater.* **33**, 1984–1988 (2011)
- Uma, T., Lzuhara, S., Nogami, M.: Structural and proton conductivity study of  $\text{P}_2\text{O}_5-\text{TiO}_2-\text{SiO}_2$  glasses. *Ceram. Soc.* **26**, 2365–2372 (2006)

**Publisher's Note** Springer Nature remains neutral with regard to jurisdictional claims in published maps and institutional affiliations.